Archives of Hydro-Engineering and Environmental Mechanics
Vol. 56 (2009), No. 3–4, pp. 101–120

Model of Particle-Particle Interaction for Saltating Grains in Water

Włodzimierz Czernuszenko

Institute of Geophysics, Polish Academy of Sciences
01-452 Warszawa, Ks. Janusza 64, Poland,
e-mail: wczer@igf.edu.pl

(Received April 02, 2009; revised September 23, 2009)

Abstract

A model of particle-particle interaction for bed sediment-laden flows, based on impulse equations, is presented. The model is applicable to dense flows in which particle motion is dominated by collisions. The model takes into account the possibility of sliding during the collision process. However, particle rotation is not considered in this model. The governing equations do not incorporate dimension of angular momentum. To verify this model, calculation of post-collision velocities was performed for several different collision simulations. The term of particle-particle interaction is implemented into a general Lagrangian model of trajectory of a sediment grain in a fluid flow. This general Lagrangian model is written according to Newton's second law; the rate of change of momentum of a particle is balanced against the surface and body forces.

Key words: Lagrangian model; saltation; particle motion; dense flow; particle collision

Notation

D	–	particle size (diameter),
e	–	coefficient of restitution,
f	–	coefficient of friction,
F_a	–	added mass force,
F_b	–	Basset force,
F_d	–	drag force,
F_g	–	Archimedes force,
F_l	–	lift force,
$\mathbf{F}_{pc}$	–	force exerted on saltating particle by another particle during collision,
g	–	gravitational acceleration,
H	–	water depth,
$\mathbf{J}$	–	impulsive force exerted on the particle,

m – mass,
n – unit normal vector directed from particle 1 to 2 at the moment of contact,
$\mathbf{n} \cdot \mathbf{V}$ – dot product of vectors $\mathbf{n}$ and $\mathbf{V}$,
t_{mft} – the mean free time,
t_{up}, t_{dw} – mean free time when particle is moving upward, and downward,
$\mathbf{V}^0, \mathbf{V}$ – relative velocities between particles before and after collision,
v – particle mean velocity.

α – collision angle,
Θ_{in} – incidence (impact) angles,
Θ_{out} – takeoff angle,
ρ – density of fluid (water),
ρ_s – density of sediment,
τ – shear stress tensor,
τ_c – critical shear stress.
ν – kinematic viscosity,

Subscripts

f – fluid phase,
mft – mean free time,
n – normal component,
s – sediment,
t – tangential component,
$1, 2$ – refer to the velocity of two particles.

Superscript

0 – values before collision.

1. Introduction

Bedload sediment can be transported in several ways. A grain begins to move by rolling over the surface of the bed, but with a slight increase in boundary shear stress, this grain hops up from the bed and follows a ballistic-like trajectory. This latter motion is called saltation, and it is considered to be the dominant mode of bed-load transport (Sekine and Kikkawa 1992). Bagnold (1956) described saltation as the unsuspended transport of particles over a granular bed by a fluid flow, in the form of consecutive hops within the near-bed region. It is governed mainly by the action of hydrodynamic forces that carry the particles through flow, the downward pull gravity and the collision of the particles with the bed, which transfer their streamwise momentum into upward momentum, thus sustaining the saltation motion.

The behavior of discrete particles (sand grains) in a near-bed region of turbulent flows is considered under equilibrium conditions, i.e. particles of sand grains are carried by the flow without net erosion and deposition. This behaviour results in a constant concentration of particles in time, i.e. concentration depends only on distance from the bed. The particle trajectory in turbulent flow in an open channel depends largely on the concentration of particles and their sizes. At great particle concentration there is interaction between the particles through collisions, and at relatively large sand particle sizes the resulting force is significant in the balance of all forces exerted on the particle.

A number of researchers have worked on modelling of grain saltation in water, e.g. Van Rijn (1987) and (1990), Wiberg and Smith (1985) and (1989), Sekine and Kikkawa (1992), Nino and Garcia (1996). Some of these studies have been concerned with the saltation of gravel and others the saltation of sand. All these models are based on the Lagrangian equation governing particle motion and on deterministic or stochastic approaches for estimating the initial conditions. This equation is written according to Newton's second law, i.e. the rate of change of momentum of a particle is balanced against the surface and body forces acting on it. All forces exerted on the moving particle in turbulent flows in the vicinity of the bed are steady-state drag forces, pressure gradient and buoyancy forces, unsteady forces (virtual mass and Basset forces), lift forces (Saffman and Magnus forces) and some body forces. So far, the force responsible for particle-particle interactions – $\mathbf{F}_{pc}$, which is very important, especially in the dense flow – has not been taken into account. There is no doubt that in the vicinity of the bed, particle motion is controlled by collision; therefore this force should be taken into account. Particle-particle interaction (collision) can be neglected only in dilute flows, when the concentration is less than 10^{-3}, i.e. in the one- or two-way coupling regimes (Elghobashi 1994). The dense flow, belonging to a four-way coupling regime, is one in which particle motion is controlled by collisions.

Herein, a model of particle–particle interaction is presented which is based on the physically fundamental principle of the impulse equation, for particles before and after collisions. It allows for constructing a new force responsible for collision between particles as well as for formulation of a new initial condition built on well-defined principles related to not only the geometry of particle-particle interaction but also on the principles of physics of particle collisions. It is shown how to adopt the model to get conditions at which the saltation of sediment particles can be a continuous process (Lee et al 2000). In this study only simple binary collisions are considered, along with collisions that take place in a very short time, in absence of any external force between two particles, i.e. the hard sphere model. The particles are assumed to be uniform both in shape and size. To adopt the collision model to describe the saltation movement of a single grain moving within the bedload, the mean free time of a particle is considered.

2. Mean Free Time of Discrete Particles in Water Flows

A particle trajectory is considered in a steady and uniform (two-dimensional) flow under the equilibrium condition, i.e. the same amount of sediment is eroded as deposited. This results in a constant concentration of particles in time, i.e. concentration depends solely on distance from the bed. Visualizations of the particle motion in the near-bed region showed that a particle is picked up from the bed, lifts away from the bed through some kind of ejection events, and is then deposited back to the bed. During this motion, the particle collides with other particles losing some energy, which modifies the particle trajectory. The average time between collisions with other particles is called the mean free time, and the average distance between collisions is the mean free path. The relation between these two mean quantities is considered in statistical physics (see i.e. Reif 1967). We are limited here to calculating the mean free time only to an approximate degree. Let us consider two particles, particle 1 and 2 approaching each other with relative velocity **V**, in the vicinity of the bed where sediment particles are in equilibrium. Based on simple geometrical examination it is possible to show that the collision occurs if the following relationship is fulfilled

$$\pi d^2 \left(\left| \overline{\mathbf{V}} \right| t_{mft} \right) n = 1, \tag{1}$$

where d is the diameter of spherical particle (πd^2 is the effective cross section for collision), $\left| \overline{\mathbf{V}} \right|$ is the absolute value of relative velocity particles, $t_{mf}t$ is the mean free time and n is the number of particles per unit of fluid volume (concentration). Then, it is easy to calculate the mean free time from Eq. (1).

$$t_{mft} = \frac{1}{n \, \pi \, d^2 \left| \overline{\mathbf{V}} \right|}. \tag{2}$$

The mean free time is small when the concentration and the size of particles are large, likewise when the average relative velocity of particles is high because then collisions may occur more frequently at the same concentration of particles.

3. Model of Particle-Particle Interaction

The movement of sand grains in the bed vicinity is controlled by collisions with other moving grains or with grains comprising the bed. During the collision process the force is very large but acts in a rather short time, therefore it is difficult to control. It is much easier to control the product of force and time of collision by applying the impulse force as the measure of change of momentum. This approach is used in this paper.

The flow in which particle motion is controlled by collisions is called dense flow. In this kind of flow, the ratio of momentum response time of particle – t_r to

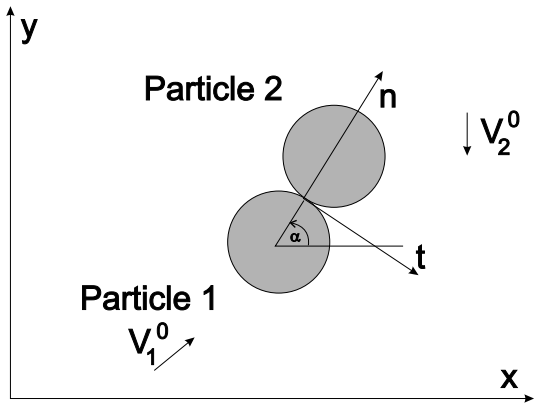

Fig. 1. Particle-particle collision. Spherical particles 1 and 2 with masses m_1 and m_2 at the moment of collision; **n** and **t** are unit orthogonal vectors located at the point of contact; v_1^0 and v_2^0 the initial velocities before collision

the mean free time between collisions – t_{mft} should exceed unity, i.e., $t_r/t_{mft} > 1$. The momentum response time is the time required for the particle released from the rest to achieve 63% of the free stream velocity (Crowe et al 1998). In other words, the particle has no time to respond to fluid dynamic forces before the next collision occurs. In further course, it will be assumed that particles of sand have spherical shape and constitute the disperse phase, i.e., particles are not connected. Hence it is possible to consider only simple binary collisions, not multiple collisions.

3.1. Equations for Impulse Force

It is assumed that the particles are rigid spheres and all the collisions take place in a very short time; hence all external forces can be neglected, and impulse equations are considered in place of momentum equations. Where particles are assumed to be rigid spheres, the impulse equations (without angular momentum) are given as (see Fig. 1):

$$m_1(\mathbf{v}_1 - \mathbf{v}_1^0) = \mathbf{J}; \quad m_2(\mathbf{v}_2 - \mathbf{v}_2^0) = -\mathbf{J} \tag{3}$$

where **J** is the impulsive force exerted on particle 1, the force **−J** acts on particle 2 as the reaction force. The subscripts 1 and 2 refer to the two particles and the superscript 0 denotes the values before collision. The following assumptions are made:

1. Particle deformation is neglected.
2. The friction on sliding particles obeys Coulomb's friction law.
3. Particles are hard (rigid) spheres.

4. The angular momentum of particles is neglected.

The relative velocity vectors between particles before and after collision are defined as

$$\mathbf{V}^0 = \mathbf{v}_1^0 - \mathbf{v}_2^0; \quad \mathbf{V} = \mathbf{v}_1 - \mathbf{v}_2. \tag{4}$$

The relationship between the pre and post-collisional velocities is obtained using the coefficient of restitution. For spherical elements the restitution coefficient e is defined as the ratio of the pre-collisional and post-collisional velocities, i.e.:

$$\mathbf{n} \cdot \mathbf{V} = -e\left(\mathbf{n} \cdot \mathbf{V}^0\right), \tag{5}$$

where $\mathbf{n} \cdot \mathbf{V}$ is *dot* product of vectors, $\mathbf{n}$ is the unit normal vector from particle 1 to particle 2 at the point of contact, $\mathbf{V}^0$ and $\mathbf{V}$ are the relative velocities between particles before and after collision.

It is easy to obtain the relationship for post-collision velocities from Eqs. (3)–(5):

$$\mathbf{V} = \mathbf{V}^0 + \left[\frac{(m_1 + m_2)}{m_1 m_2}\right]\mathbf{J}. \tag{6}$$

The normal component of the impulsive force, J_n exerted on particle 1 is given as

$$J_n = -\left[\frac{m_1 m_2}{(m_1 + m_2)}\right](1 + e)(\mathbf{n} \cdot \mathbf{V}^0). \tag{7}$$

Assuming that the particles slide during the collision process, then the tangential component of the impulsive force appears and from Coulomb's law for friction, is equal to

$$J_t = f J_n, \tag{8}$$

where f is the friction coefficient.

The absolute value of impulse force is

$$J = \sqrt{\left(J_n^2 + J_t^2\right)} = J_n \sqrt{(1 + f^2)}. \tag{9}$$

Note again that all above equations are developed on the basis of two impulsive force equations without impulsive torque equations. This means that the rotations of colliding particles are not taken into account.

3.1.1. Examples of Calculation of the Impulsive Force in the Collision of Particles

The main aim of these calculations is to show the influence of the restitution coefficient as well as the friction force between two colliding particles on the impulsive

force exerted on particle 1 by particle 2. The collisions are performed for two identical, spherical particles: particle 1 is entrained by flow at the angle equal to 27 degrees, a while the falling particle (particle 2) travels downwards vertically, i.e. the particles move with pre-collisional velocities $v_1^0 = (0.89, 0.45)$ and $v_2^0 = (0, -1)$. These particles can collide at a contact point ranging from 0 to 180 degrees. This location of the contact point is defined by the angle α between a unit vector $\mathbf{n}$ directed from particle 1 to particle 2 and the horizontal x-axis (Fig. 1).

The easiest case is related to collisions without shear force ($f = 0$) between particles, i.e. impact without any slide between particles during the collision process. In this case the normal component of the impulsive force exerted on particle 1 is simplified to the form

$$J_n = -\left(\frac{m}{2}\right)(1 + e)\left(\mathbf{n} \cdot \mathbf{V^0}\right). \tag{10}$$

It is easy to see the role of the restitution coefficient, which is always less than one and shows how the impulsive force is reduced by the collision. To show the role of friction in the process of collision, collisions between particles with and without friction were considered and results are shown in Fig. 2.

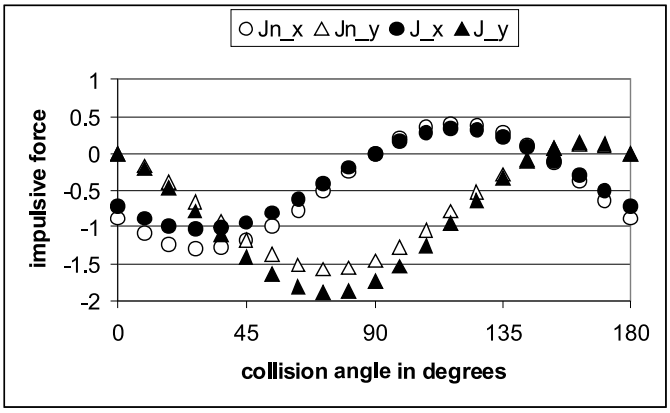

Fig. 2. The components of the total impulsive force for collisions of two particles with restitution coefficient $e = 1$, and without friction force, as a function of different contact angles ($J_{n,x}$, $J_{n,y}$), and for collision with friction force ($f = 0.2$) (J_x, J_y). For both cases velocities before collision are: $v_1^0 = (0.89, 0.45)$, $v_2^0 = (0, -1)$. Note on the units: if velocity is expressed in m/s and mass in kg, then the impulse force is expressed in Ns, but if velocity is expressed in mm/s and mass in grams, then the impulse force is expressed in 10^{-6} Ns

The role of the tangential component of the impulsive force in the process of collision is shown by comparison of the total impulsive force, with and without friction, during the collision of two particles (Fig. 2). The forces acting on spherical particles during their collision depend on the angle of collision. The components of these forces for collision without friction force (J_{n_x}, J_{n_y}), and with friction

($J_{\_x}$, $J_{\_y}$) are shown in Figure 2 as a function of collision angle. The maximum for impulsive forces J_n between particles appears at $\alpha = 58.5°$ (this is the case when vectors $\mathbf{V}^0$ and $\mathbf{n}$ are parallel to each other). It is clear that for $\alpha = 90°$ the horizontal component of impulsive force $J_{n,x}$ changes its sign from negative to positive.

3.2. Equations for Velocities

To verify the model, calculations of post-collision velocities for different angles of collisions for both particles are performed. Substituting the components of the impulse force (Eqs. (7) and (8)) into impulse equations (3) gives the two formulae for post-collisional velocities, as

$$\mathbf{v}_1 = \mathbf{v}_1^0 - (\mathbf{n} - f\mathbf{t})\left(\mathbf{n}\mathbf{V}^0\right)(1+e)\frac{m_2}{(m_1+m_2)}, \tag{11}$$

$$\mathbf{v}_2 = \mathbf{v}_2^0 + (\mathbf{n} - f\mathbf{t})\left(\mathbf{n}\mathbf{V}^0\right)(1+e)\frac{m_1}{(m_1+m_2)}, \tag{12}$$

where $\mathbf{v}_1$ and $\mathbf{v}_2$ are post-collision velocity vectors of particles 1 and 2, respectively.

3.2.1. Post-collisional Velocities in the Case of Particle-Particle Interaction

To show how the model works, the post-collision velocities of two spherical particles colliding at different contact (hitting) points are calculated. Particles with the same mass are moving with pre-collision velocities $v_1^0 = (0.89, 0.45)$, $v_2^0 = (0, -1)$ and they collide with friction force as well as without friction force. The first particle represents the entrained particle with an ejection angle equal to 27 degrees, while the second particle is the falling one. Both particles collide at different collision points defined by angle α (see Fig. 1). Figure 3 shows the post-collision velocities of two particles after perfect collisions without friction ($f = 0$) and restitution coefficient $e = 1$, and Figure 4 shows the post-collision velocities with friction and restitution coefficient $e = 0.6$.

Figure 3 displays the resulting velocities after perfect collision, i.e. collision in which momentum is preserved. It is easy to see the perfect momentum exchange between the components of velocities. For $\alpha = 0°$ the whole x-momentum of particle 1 before collision is transferred to particle 2. Particle 1 changes its horizontal velocity from negative to positive at the hitting angle ca 58.5° and it reaches its maximum at $\alpha = 117°$. It moves vertically in the negative direction for hitting angles in the range of (20°, 127°). Particle 2 moves in the positive x-direction for collision angles $\alpha \in (0°,\ 90°)$, but at 90° it changes its sense to the negative one.

As an example, Figure 4 displays post-collision velocities after the collision defined by initial pre-collision velocities $v_1^0 = (0.89, 0.45)$, $v_2^0 = (0, -1)$, the restitution coefficient $e = 0.6$ and friction coefficient $f = 0.2$. Now, at $\alpha = 0°$ the whole x-momentum of particle 1 prior to the collision is transferred to both particles. This is the effect of the occurrence of friction. For all other collision angles, the initial,

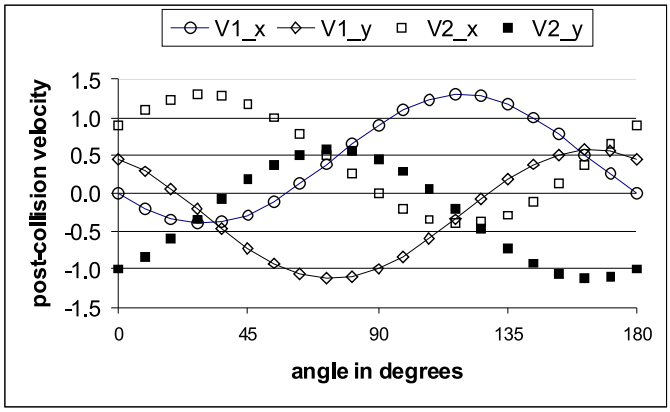

Fig. 3. Components of post-collision velocities for both particles after perfect collision ($e = 1$ and $f = 0$) and for initial velocities (before collision) $v_1^0 = (0.89, 0.45)$, $v_2^0 = (0, -1)$. $(V1\_x, V1\_y)$ and $(V2\_x, V2\_y)$ are velocities of particles 1 and 2, respectively. Note on units: post-collision velocities have the same units as the initial velocities (usually they are mm/s or cm/s)

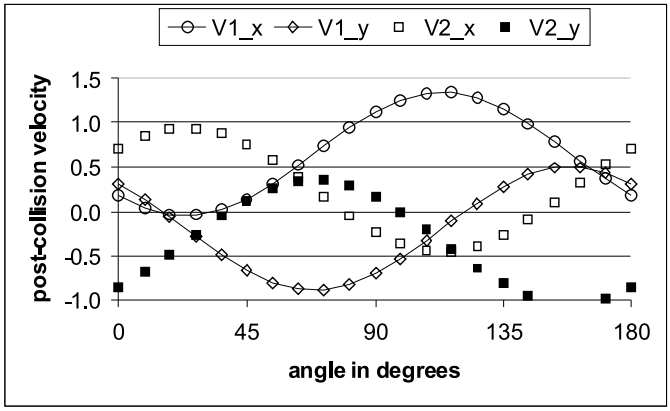

Fig. 4. Components of the post-collision velocities for both particles for $f = 0.2$ and $e = 0.6$ and for initial velocities (before collision) $v_1^0 = (0.89, 0.45)$, $v_2^0 = (0, -1)$. $(V1\_x, V1\_y)$ and $(V2\_x, V2\_y)$ are velocities of particles 1 and 2, respectively. For velocity units see Figure 3

total x- and y-momentum are divided between the two particles depending on the angle of collision. The x-component of velocity for particle 1 is positive for almost all collision angles, and the maximum is reached at the same angle as for the perfect collision $\alpha = 117°$. Particle 2 moves in the positive direction for the collision angles $\alpha \in (0°,\ 80°)$, which means less than in the case of perfect collision.

4. Collision at the Bed

4.1. Basic Definitions

Particle-bed interaction is defined by the particle collision angle, the particles' velocities before collision, the properties of the particle and bed materials, the particle shape, and the roughness of the bed. The collision angle is determined by the particle trajectory and the geometry of the bed. The restitution and friction coefficients depend on the properties of the particle and bed materials. The roughness of the bed is represented by the height of bed elements interferred with the flow and it is defined by the Nikuradse concept of logarithmic velocity profile. There are a few approaches to modelling particle-bed collision, see for example Lee et al (2006), Nino and Garcia (1998), Lukerchenko et al (2006).

Here, it is assumed that uniformly packed spheres form the bed, as shown in Figure 5 by grey spheres equal in size to transported particles. The bed is not able to erode, therefore it is assumed that the mass of the spheres which constitute the bed are much heavier, say 500 times the mass of the flowing particles. Thus, the post-collision velocity of bed particles is negligibly small and can be omitted from our considerations. For example, if the impact velocity is 1 cm/s, the velocity of the bed particle will be 0.05 mm/s at the most. Of course, it is possible to assume much heavier particles constituting the bed.

Consider a case where particle 1 is falling down with velocity $\mathbf{v}_1^0$ and striking particle 2 which is located on the bed, i.e. $\mathbf{v}_2^0 = (0,\ 0)$. If the bed consists of uniformly packed spherical particles, the flowing particle is not able to strike the bed particle at collision angle smaller than 60 nor greater than 120 degrees due to the proximity of neighboring particles (see dark grey spheres in Fig. 5). The possible, maximum range of the collision angle is dependent on the impact velocity vector and the geometry of the particle, for a spherical particle, this is equal to (60^o, 120^o) (see Fig. 5). Definitions of incidence and other angles are given in Figure 6.

When the impact (incidence) velocity vector is inclined to the horizontal axis at angles smaller than 30^o, then it is easy to show that the minimum collision angle varies linearly with respect to the incidence angle, and maximum collision angles can be calculated from the following formula (Rowiński and Czernuszenko 1999)

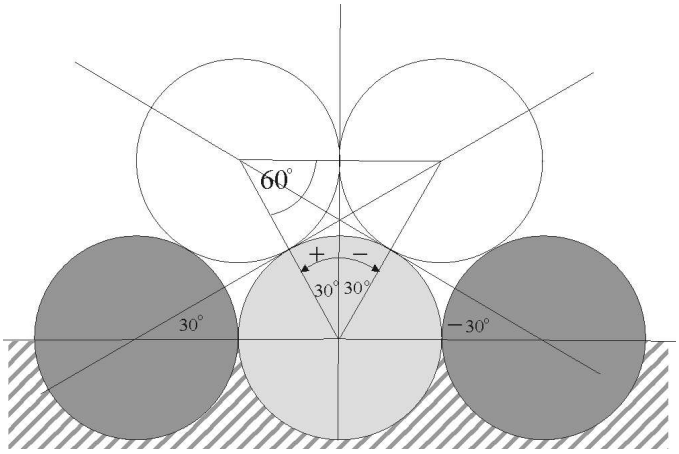

Fig. 5. The largest range for collision angles between two extreme locations of falling down particle (the white spheres) and the bed-particle (the light grey sphere) is (60°, 120°) for the incidence angle θ_{in} from (30°, 90°). If θ_{in} is from the range of (0°, 30°), the range of possible collision angle is much less

$$\tan\ (\alpha_{\max} - 90^\circ) = \frac{a\sqrt{1+a^2} + \sqrt{a\left(-a - 2\sqrt{1+a^2}\right) + a^2}}{a - a\sqrt{a\left(-a - 2\sqrt{1+a^2}\right)} + \sqrt{1+a^2}}, \tag{13}$$

where $a = -\tan(\theta_{in})$ and $0 < \theta_{in} < 30$.

All ranges of the collision angle as a function of impact angles are displayed in Fig. 7 for the perfect collision. All angles are in degrees.

4.2. The Splash Function

The main features of particle-wall interaction allow us to construct the initial condition for particle collision at the bed in the case of continuous saltation process. Below is a proposed procedure that can be used to formulate the initial condition for modeling of saltating sediment particles in bed-sediment laden flows.

Let us assume that particle 1 approaches any bed particle at the incidence angle. It is not possible to predict the collision angle, therefore a stochastic model proposed by Nino and Garcia (1994) is used to determine the probability distribution of the collision angle α. A conditional probability density function of the collision angle for a given incidence angle Θ_{in} – $p(\alpha|\Theta_{in})$ is assumed to be uniform, which is equivalent to assuming that the particle considered has a uniform probability of being located anywhere in the bed. Knowing the incidence angle, the range of collision angles is determined from Figure 7. Next, the collision angle is determined with the use of a random number generator. Having known the collision angle, we

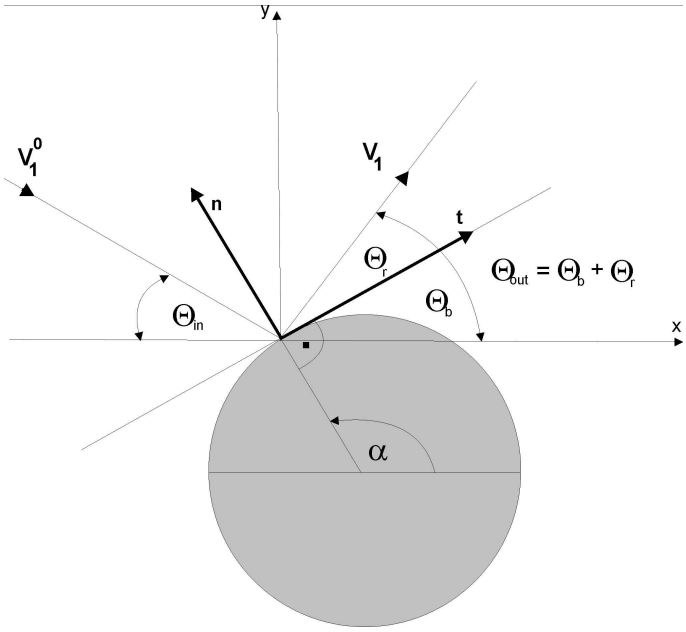

Fig. 6. Collision angles and the coordinate system in the case of simple collision of flowing particle with one spherical bed particle (the light grey sphere), where α is angle of collision, Θ_b is angle between horizontal and hypothetical repulsion plane, Θ_r is angle of response i.e. the angle between the hypothetical repulsion plane and takeoff velocity vector, Θ_{in} is the incidence (impact) angle of flowing particle, i.e. an angle between x-axis and velocity vector V_1^0, ($0° < \Theta_{in} < 90°$), Θ_{out} = angle of takeoff, i.e. an angle between x-axis and velocity vector V_1, $\Theta_{out} = \Theta_b + \Theta_r$ and two velocities: V_1^0, V_1 are velocity vectors before and after collision, respectively

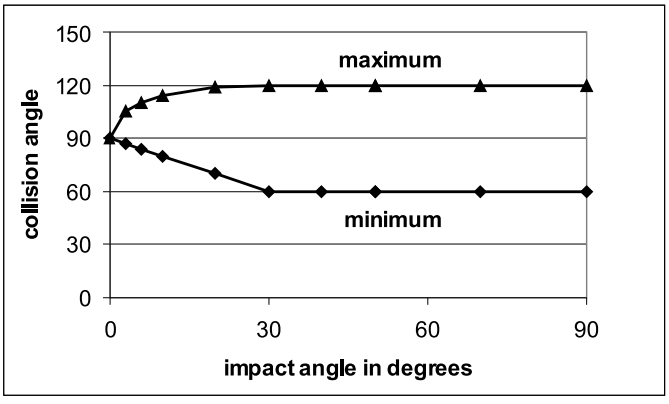

Fig. 7. Maximum and minimum collision angles as a function of the incidence angles

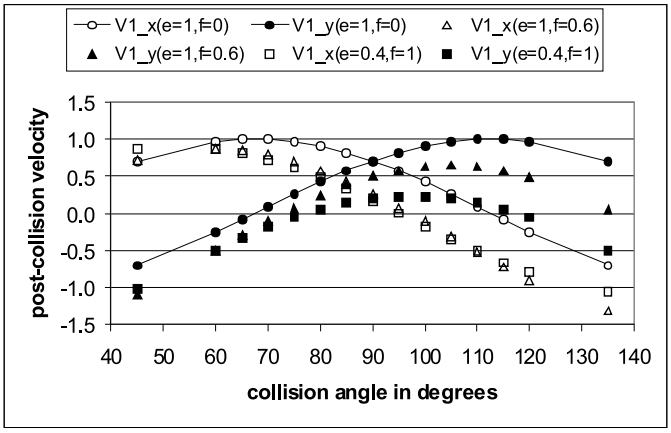

Fig. 8. Post-collision particle velocity in the case of a particle striking a channel bed formed of very heavy particles. The collision takes place at the impact velocity $(0.707, -0.707)$, two different restitution coefficients ($e = 1, e = 0.4$) and two friction coefficients ($f = 0, f = 0.6$). Note on units: post-collision velocities have the same units as the initial velocities (usually they are mm/s or cm/s)

calculate the rebound velocity and define the initial condition, i.e. initial velocity of particle for the next hop.

4.3. Conditions for the Continuous Saltation

To keep saltation as a continuous process, the post-collision velocity should be positive and should exceed the velocity entrainment limit. Because the velocity limit is unknown, it was assumed that the velocity is equal to any small positive number. The post-collision velocity depends on the friction and restitution coefficients and is displayed in Figure 8 for the given incidence angles. This figure presents the results of calculations of post-collision velocities based on Eqs. (11) and (12) as a function of the collision angle. The results of calculations of the post-collision velocities of particle 1, falling downwards with velocity $\mathbf{v}_1^0 = (0.707, -0.707)$, striking the bed particle without friction ($f = 0$) and with the friction ($f = 0.6$) and with two restitution coefficients ($e = 1$ and $e = 0.4$), are presented in Figure 8.

One can observe the role of both coefficients in calculations of the possible range of collision angles at which continuous saltation occurs. This range depends on the restitution and friction coefficients. One can read from Figure 8 that for perfect collision ($e = 1$, $f = 0$) the range is (70°, 110°), for case ($e = 1$, $f = 0.6$) the range is (75°, 95°) and for case ($e = 0.4$, $f = 0$) the range is (80°, 93°). It is apparent that even for perfect collision, the range of collision angles is reduced in comparison with the theoretical one, i.e. (60°, 120°).

The plot of post-collision velocities vs. collision angles is also a function of the incidence angle of the sediment particle. Figure 9 shows the role of the inci-

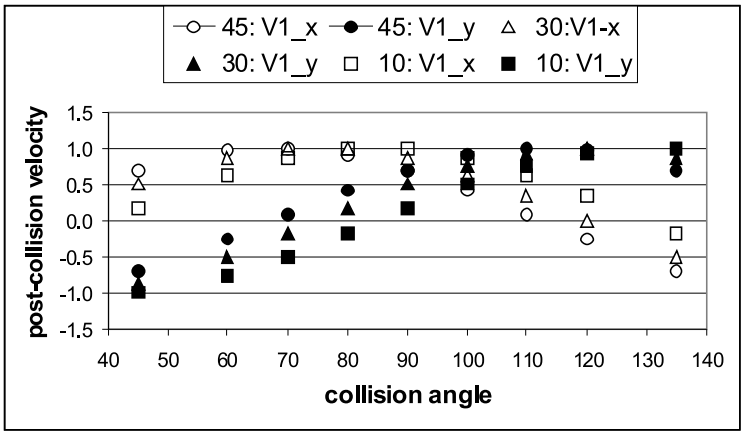

Fig. 9. Post-collision particle velocity vs. collision angle for a particle striking the channel bed. The bed is formed by particles much heavier than flowing particles. All calculations were made for perfect collision ($e = 1, f = 0$) and for the three impact velocities: (0.707, −0.707), (0,866, −0.5) and (0.984, −0.173), i.e. three incidence angles: 45°, 30° and 10°. For velocity units see Figure 8

dence angle in calculations of the post-collision velocity vs collision angles. It also shows the role of the incidence angle in calculations of the possible range of the collision angle at which continuous saltation could occur. This range depends on the incidence angle, and from Figure 9 one can read that for the perfect collision ($e = 1, f = 0$) and the impact velocity (0.707, −0.707) (incidence angle = 45°) the range is (70°, 110°). Similarly, one can read that for the incidence angle 30° the range is (77°, 118°), and for the incidence angle 10° the range is (87º, 128°). Summarizing the results of the above calculations, one can say that if the incidence angle varies from 45 to 10 degrees, the range of possible collision angles is reduced by almost 20 degrees.

It is interesting to note that the above-discussed process of perfect collision agrees with typical results of the collision of two elastic balls, see Figure 9 for three collision angles i.e. 45°, 90° and 135°. For two extreme collision angles, one can observe that for 45° the post-collision velocity remains the same; but for 135° this velocity only changes its sign. For 90°, only the vertical component of post-collision velocity changes its sign.

The role of the incidence angle in calculations of the possible range of collision angles at which continuous saltation could take place is depicted in Figure 10. Continuous saltation is possible only when the takeoff angle is positive. This condition is equivalent to the above-mentioned condition, which is expressed in terms of post-collision velocity. Figure 10 shows at which incidence and collision angles the takeoff angle is a positive one, e.g. under which conditions (incidental and collision angles) continuous saltation occurred.

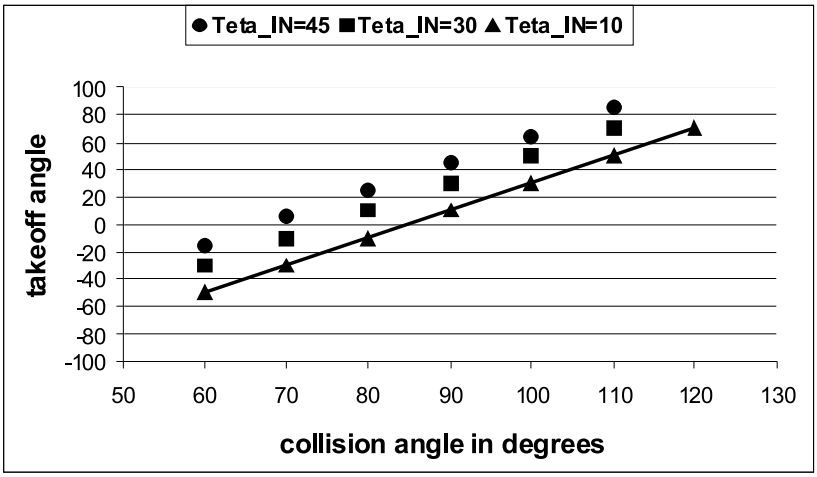

Fig. 10. The takeoff angle vs. the collision angle in degrees for different incidence angles Θ_{in} (in legend Teta_IN) for the case of perfect collision

4.4. Measurements of Particle Collision with the Bed

Nino and Garcia (1998) observed the saltation of sand (mean diameter of about 0.5 mm) in an open channel flow by using a high-speed video system. The typical jump was about 8–12 particle diameters (D) in length with maximum heights of about 1.3–1.8 D. The angles of incidence and takeoff, measured with respect to a line parallel to the channel bed are not correlated and vary in ranges of (0°, 45°) and (0°, 80°), respectively.

Nino et al (1994) used the same techniques to observe the saltation of natural gravel particles (15 mm and 31 mm) in a steep, movable-bed channel. The mean saltation length and height as functions of the ratio τ_*/τ_{*c} (dimensional shear stress/ dimensional critical shear stress) are about 5–7 particle diameters (D) and 1–2 D, respectively. It is worth noting that higher values are received for the smaller particles, i.e. 15 mm. Results of the impact and takeoff angles are the same as obtained by Nino and Garcia (1998), i.e. they are not correlated and vary in ranges (0°, 45°) and (0°, 80°), respectively.

There is some controversy regarding the possibility of the continuous saltation process (collision-rebound process), e.g. Abbott and Francis (1977) deny such a possibility, while Nino and Garcia (1998) try to prove that the collision-rebound process is possible. The presented model for collisions of spherical hard particles gives us conditions under which the saltation of sediment sphere may be a continuous process. There is one reasonable condition for this, i.e. post-collision velocity should be directed upwards and exceed the velocity entrainment limit. If it is assumed that the velocity limit is equal to any small positive number or if we know this limit, then for given the impact velocity based on:

– Figures 8, one could read the positive sign of post-velocity components for the range of the collision angle for the friction and restitution coefficients,
– Figure 9, one could read the positive sign of post-velocity components for the range of the collision angle for chosen of the incidence angle,
– Figure 10, one could read the positive sign of the takeoff angle for the range of the collision angle for the chosen of the incidence angle.

All these Figures along with the consequences arising from them are discussed in detail in Section 4.2. Now, one could say that in order to keep saltation as a continuous process, the range of the collision angle should be narrowed in comparison to the theoretical one discussed in Section 4.1.

5. A Theoretical Model for Saltating Grain in Water

The slow motion of a spherical particle in a fluid may be described by Newton's equation in the following form (Hinze 1975)

$$m_s \frac{d\mathbf{v_s}}{dt} = \mathbf{F_g} + \mathbf{F_d} + \mathbf{F_l} + \mathbf{F_m} + \mathbf{F_a} + \mathbf{F_b} + \mathbf{F_{pc}}, \tag{14}$$

where:

m_s – mass of the solid particle (sediment) in water flow,
$\mathbf{v_s}$ – velocity of the particle (grain) along the bed in the water stream,
$\mathbf{F_g}$ – gravitation force or buoyancy force,
$\mathbf{F_d}$ – drag force acting on the particle in a uniform pressure field when there is no acceleration the relative velocity between the particle and the conveying fluid,
$\mathbf{F_l}$ – lift force acting on a particle due to particle rotation. The rotation may be caused by a velocity gradient or may be imposed from some other source. The Saffman lift force is due to the pressure distribution developed on a particle due to the rotation induced by a velocity gradient. The higher velocity on the top of the particle gives rise to a low pressure, and the high pressure on the low velocity side gives rise to a lift force,
$\mathbf{F_m}$ – the Magnus force is the lift developed due to rotation of the particle. The lift is caused by a pressure difference between both sides of the particle resulting from the velocity differential due to rotation. The rotation may be caused by a source other that the velocity gradient,
$\mathbf{F_a}$ – force representing virtual or apparent mass effect. This force relates to the force required to accelerate the surrounding fluid. This force can be categorized as one of the unsteady forces. The other unsteady force is the Basset force,

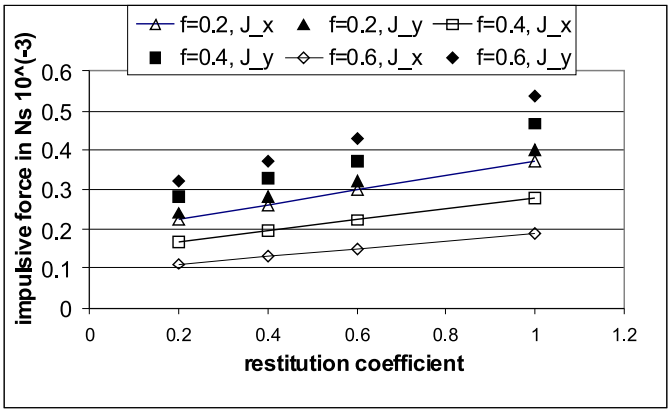

Fig. 11. Average impulsive force defined by Eq. 15 as functions of the friction coefficient and the restitution coefficient of two identical 1 g particles for velocities before collision: $v_1^0 = (0.89, 0.45)$, $v_2^0 = (0, -0.25)$ [m/s]

- $\mathbf{F_b}$ – the Basset force accounts for the viscous effects due to acceleration. The value of the Basset force depends on the acceleration history up to the present time. This force is difficult to evaluate and is usually negligible for slow water velocity,
- $\mathbf{F_{pc}}$ – force exerted on a saltating particle from another particle during collision.

Eq. (14) will be used as the model for the saltation motion of a sediment particle in an open channel flow. There is no doubt that in the vicinity of the bed, particle motion is controlled by collision; therefore the force responsible for particle-particle interactions ($\mathbf{F}_{pc}$) should be taken into account. The force $\mathbf{F}_{pc}$ can be described in the following way.

If the location of collision contact and the velocities of both particles before collision are known, there is no problem to define the force responsible for collision. Usually, the location of contact point is not known, even it is impossible to predict it. Therefore, it is assumed that the location of the contact point is a random function with a uniform probability distribution in the range of angles from 0 to π; thus the mean impulsive force can be calculated for the chosen velocities as

$$\overline{J} = \frac{1}{\pi}\int_0^{\pi} (J_x, J_y)\, da = \left(\frac{1}{\pi}\int_0^{\pi} J_x\, da,\ \frac{1}{\pi}\int_0^{\pi} J_y\, da\right). \tag{15}$$

The averaged impulsive force Eq. (15) depends on friction and restitution coefficients, as depicted in Fig. 11.

The average impulsive force between two identical particles, defined by Eqs. (15), (9) and (7), varies linearly with the mass of the particle, as does the restitution

coefficient. If it is assumed that there are n collisions during the upward movement of a particle and the same number in the opposite direction, then the mean force acting on the chosen particle during the whole hop of the particle ($t_{up} + t_{dw}$), takes the form

$$\overline{\mathbf{F_{pc}}} = \begin{cases} \dfrac{n\bar{\mathbf{J}}}{t_{up}} & \text{for} \quad t \in t_{up}, \\ \dfrac{-n\bar{\mathbf{J}}}{t_{dw}} & \text{for} \quad t \in t_{dw}, \end{cases} \tag{16}$$

where τ_{up} and τ_{dw} are the mean times when the particle is moving upward and downward, respectively, and it is assumed that they are equal to each other.

6. Summary and Conclusions

The model of particle-particle interaction was developed on the basis of impulse equations for hard spheres and the relationship between the pre- and post-collision velocities. This takes into account the friction force and loss of energy during collisions, after assuming a binary two-dimensional mechanism of interaction for bed-sediment laden-flows. The force exerted on a saltating particle from another particle during collision is also developed for Lagrange equations for the motion of saltating grains in water. Some additional conditions are developed for particle collisions at the bed, especially conditions for keeping saltation as a continuous process. Numerical simulations of binary particle collisions confirmed that the obtained post-collision velocities agree with our current knowledge on the collisions of two hard, elastic balls. Further work is required to define more precisely the empirical coefficients such as the restitution coefficient as well the friction coefficient between particles in turbulent boundary layer flows. One can draw the following conclusions from simulations:

1. The model of particle-particle interaction describes the impulsive force for the given pre-collision velocities as a function of the angle of collision. The force depends on the angle of collision, the friction and restitution coefficients. The latter causes the decrease in the impulsive force exerted between particles. The friction coefficient creates the tangential component of the impulsive force, i.e. the component that is responsible for sliding between particles during the collision process.
2. The post-collision velocities depend on the restitution coefficient, the friction force and the angle of collision. Generally, the total momentum of particles is conserved for perfect collisions for all collision angles. The restitution coefficient attenuated the post-collision velocities, and the friction coefficient causes some changes in maximum velocities as well as in their location.

3. The model allows for formulating the correct boundary conditions in the case of particle-wall interaction as a function of given incidental angles when uniformly packed spheres constitute the bed. Furthermore, it allows us to keep saltation as a continuous process for collision with different friction and restitution coefficients.
4. The takeoff angle of the post-collision velocity can be presented as the function of two angles: impact and collision angle. Knowing this function, it is possible to construct the boundary condition for a continuous saltation process.

Acknowledgments

This work was financially supported by The Ministry of Higher Education and Science, Grant TROIANET. The author wishes to express his thanks to Dr P. Rowiński for reviewing an early draft of the results and contributing helpful criticism. Also, he appreciates the assistance of Mr Robert Bialik in the analysis and plotting of the same data.

References

Abbot J. E. and Francis J. R. D. (1977) Saltation and suspension trajectories of solid grains in a water, *Philos. Trans. R. Soc. London* A., 284, 225–254.

Bagnold R. A. (1956) The flow of cohesionless grains in fluids, *Phil. Trans. R. Soc.* London A, 249, 235–297.

Crowe C., M. Sommerfeld and Y. Tsuji (1998) *Multiphase Flows With Droplets and Particles,* CRC Press, Boca Raton.

Elghobashi S. (1994) On Predicting Particle-Laden Turbulent Flows, *Applied Scientific Research*, **52** (4), 309–329.

Hinze J. O. (1975) *Turbulence*, McGraw-Hill Inc., New York.

Lee H.-Y. et al (2000) Investigations of continuous bed load saltating process, *Journal of Hydraulic Engineering*, **126** (9), 691–699.

Lee H.-Y., Lin Y.-T., You J.-Y. and Wang H.-W. (2006) On three-dimensional continuous saltating process of sediment particles near the channel bed, *Journal of Hydraulic Research,* **44** (3), 374–389.

Lukerchenko N., Chara Z. and Vlasak P. (2006) 2D Numerical model of particle-bed collision in fluid-particle flows over bed, *Journal of Hydraulic Research,* **44** (1), 70–78.

Nino Y., Garcia M. H. and Ayala L. (1994) Gravel saltation; 1. Experiments, *Water Resource Research,* **30** (6), 1907–1914.

Nino Y. and Garcia M. H. (1996) Experiments on particle-turbulence interactions in the near-wall region of open channel flow, *Journal of Fluid Mechanics*, 326, 285–319.

Nino Y. and Garcia M. H. (1998) Using Lagrangian particle saltation observations for bedload sediment transport modeling, *Hydrological Processes* 12, 1197-1218.

Reif F. (1967) *Statistical Physics: Berkeley Physics Course*, McGraw-Hill Book Company, New York.

Rowiński P. M., Czernuszenko W. (1999) Modeling of sand grain paths in a turbulent open channel flow, *Proc. 28*th *IAHR Congress*, CD-ROM, Graz, Austria.

Sekine M. and Kikkawa H. (1992) Mechanics of saltating grains. II, *Journal of Hydraulic Engineering*, **118** (4), 536–58.

Van Rijn L. C. (1987) *Mathematical Modeling of Morphological Processes,* Delft: Waterloopkundig Laboratorium.

Van Rijn L. C. (1990) *Principles of Sediment Transport in Rivers, Estuaries and Coastal Seas,* Nederlandes.

Wiberg P. L. and Smith J. D. (1989) Model for calculating bed load transport of sediment, *Journal of Hydraulic Engineering*, **115** (1) 101–23.

Wiberg P. L. and Smith J. D. (1985) A Theoretical Model for Saltating Grains in Water, *Journal of Geophysical Research*, **90** (C4), 7341–7354.